Numerical analysis of the hydraulic transient process of the water delivery system of cascade pump stations

Long-bin Lu, Yu Tian, Xiao-hui Lei, Hao Wang, Tao Qin and Zhao Zhang

ABSTRACT

The aim of this study is to create a hydraulic numerical model to analyze the hydraulic transient process associated with the water delivery system of the cascade pumping stations of the Miyun Reservoir Regulation and Storage Project. Based on the characteristics of the project, which include open channels, co-dependent structures and control structures, a mathematical model of the corresponding inner boundary was established. The numerical model of transient flow was developed by combining computer simulation techniques with the one-dimensional Saint-Venant equations. This approach is suitable for the water delivery system of cascade pumping stations. This model was subsequently applied in the study area. The numerical simulation results show that the model of the hydraulic transient process yielded relatively high precision (error of less than 2 cm). The model was used to perform numerical simulations of flow regulation and emergency conditions in the water conveyance system. The study provides a practical numerical method for precisely evaluating the hydraulic transient process for the water delivery system of cascade pumping stations, basic data for the operation and optimization of the water conveyance system, and a reference for the safe operation of the Miyun Reservoir Storage Project, as well as efficient water delivery.

Key words | hydraulic numerical model, hydraulic response, Miyun Reservoir Storage Project, numerical simulation, Saint-Venant equation

Long-bin Lu
Key Laboratory of Beijing for Water Quality Science and Water Environment Recovery Engineering,
College of Architecture and Civil Engineering,
Beijing University of Technology,
Beijing 100124,
China

Long-bin Lu
Yu Tian
Xiao-hui Lei (corresponding author)
Hao Wang
Tao Qin
Zhao Zhang
State Key Laboratory of Simulation and Regulation of Water Cycle in River Basin,
China Institute of Water Resources and Hydropower Research,
Beijing 100038,
China
E-mail: *rain_fields@qq.com*

Zhao Zhang
College of Water Conservancy and Hydropower Engineering,
Hohai University,
Nanjing 210098,
China

INTRODUCTION

Water resources in China are unevenly distributed temporally and spatially, and water shortages occur in some areas (Chen *et al.* 2013). To effectively alleviate and solve regional issues associated with water resource shortages and allocation, the construction and scientific scheduling of trans-basin pumping stations are becoming increasingly important (Menke *et al.* 2016). In recent years, a number of large-scale, inter-basin, trans-regional, long-distance water conveyance projects involving cascading pump stations have been built in China. Such projects include the Jiaodong region Yellow River water diversion project in Shandong province, the Dong Shen water supply project in Guangzhou province, the Luanhe-Tianjin water diversion project in Tianjin municipality, the Yellow River diversion project in Shaanxi, phase 1 of the east route of the South-to-North Water Diversion Project, the middle route of the South-to-North Water Transfer Project, etc. (Wang *et al.* 2009; Guo *et al.* 2012). Some of the water diversion projects are characterized by large distances and complex terrain. These projects require high lifting head, a single pump station cannot meet the requirement (Sang 2012). Therefore, multi-phase, hierarchical pump station models must be developed considering the terrain and surroundings, such as those created in water conveyance projects involving cascade pumping stations (Yang 2016). Under certain operating conditions, such as shutdown, flow control and emergency

doi: 10.2166/ws.2017.198

situations, the original state of the system is disrupted, which results in an unbalanced and unsteady system state. The transition process makes parameters such as water level, velocity and discharge change considerably and can lead to a series of serious consequences (Chang *et al.* 2011; Li *et al.* 2011; Zhang & Zhang 2011; Zhang *et al.* 2014; Pudeh *et al.* 2016).

A variety of studies have been conducted regarding the simulation of hydraulic transients (unsteady flow) in water delivery systems, including theoretical analysis (Strelkoff & Clemmens 1998), prototype observations (Devries *et al.* 2014), physical modeling (Ghumman *et al.* 2012), and numerical simulation (Zhang *et al.* 2013). With the rapid development of computer simulation techniques, numerical simulation has become commonly used to study hydraulic transient processes in water conveyance systems. Various existing numerical models, such as the Unsteady State Model (USM), CARIMA model, Canal model, Duflow model and Modis model, all provide good stability and accuracy, despite their shortcomings (Zhang *et al.* 2007). However, different irrigation channels have different requirements in the models, and various existing models are not universal (Burt & Gartrell 1993). Clemmens *et al.* (2005) performed unsteady flow simulations using three commercial software packages, CanalCAD, Mike11 and Sobek, and noted that the softwares use implicit difference schemes to solve the control equations and simulate channel flow processes. This approach is characterized by high stability and precision. However, these three softwares do not include calculations for inverted siphons, aqueducts and other structures. Clemmens (2012) made a discussion about the existing canal control methods, and a new water-level control technique on the basis of water-level differences between adjacent pools was tested through simulation studies. The method is effective in controlling canal water levels when supply and demand do not match. Zhang *et al.* (2015) developed a one-dimensional unsteady numerical model of open channel by finite difference method. This model can deal with difficult inner boundaries such as gates, inverted siphons, diversion of flow, and flumes. Han *et al.* (2010) consider adopting different operating modes, as well as different gate regulation modes etc., conducting the canal unsteady flow numerical simulation with the rectangular grid characteristic method in the trapezoidal cross-section under the different gate controls. Zhao & Xu (2012) adopted a model to simulate flow in an irrigation canal and established a correlation between scattered, real-time monitoring data by superposing the 'interference flow' and input variables of the system. Gooch & Keith (2015) made a description of the USM model developed by the US Bureau of Reclamation. The field application of Staggered Net Unsteady State Model (SNUSM) has resulted in a greater degree of refinement and robustness than most generic canal unsteady state models. Bolea *et al.* (2014) developed a linear parameter-varying (LPV) model for open flow canals by means of a gray-box approach: the structure of an integral delay zero (IDZ) model is selected to obtain an LPV control model. The obtained LPV model has been tested both in a single pool and two-pool test bench canal proposed as case studies, obtaining satisfactory results in all the cases. Liu *et al.* (2013) developed a mathematical model of a canal system operated by the constant downstream depth method based on open canal hydraulics, and the results showed that this model can achieve the expected goals. Serede *et al.* (2014) studied the hydraulic characteristics of an irrigation system by using the HEC-RAS model. Due to its minimal estimation errors, the HEC-RAS model would be appropriate for evaluation of canal hydraulics steady state conditions to improve on scheme performance. Li *et al.* (2015) simulated and analyzed the canal flow and gate opening characteristics with the theory of unsteady flow and automation under different conditions. By comparison, the simulated hydraulic response characteristics at canal sections were consistent with the measured ones, and the error of canal water depth was within ± 10 cm.

In summary, this study aims to develop a numerical calculation model of transient flow that is suitable for a water delivery system based on cascade pumping stations. The model must be efficient, fast, flexible, convenient and widely applicable. The model was developed by combining computer simulation techniques and the one-dimensional Saint-Venant equations, and the suitability of the model was verified by numerical simulation of the hydraulic transient process of a water delivery system based on cascade pumping stations in the Miyun Reservoir Storage Project. The model was used to perform numerical simulations based on standard flow regulation conditions and the emergency scenarios. Additionally, the variations in hydraulic parameters such as the water

level, flow rate and flow velocity were predicted. This study not only provides the basic data for further operation and optimization of the water conveyance system but also provides a reference for safe operation of the Miyun Reservoir Storage Project, as well as efficient water delivery.

MATERIALS AND METHODS

Study area

The study area encompasses the water diverted from the South-to-North Water Transfer Project into the Miyun Reservoir Regulation and Storage Project, which spans Haidian, Changping, Huairou and Miyun counties. This area has a mid-latitude, warm, temperate continental monsoon climate and four distinct seasons. The climate is rainless and windy in spring, hot and rainy in summer, sunny and cool in autumn and cold and dry in winter. The project receives water from the Lake City Mission regulation pool of the Summer Palace and transfers water to Huairou Reservoir through the original Miyun-Beijing canal. The bottom of the channel is lined with prefabricated board, and the channel slope is complex. Along the channels, six lifting pump stations were built to increase the volume of water that can be lifted into Huairou Reservoir, with a transfer rate of 20 m^3/s (Water Conservancy Planning Design and Research Institute of Beijing 2013). The structures in the project are complex, interrelated and influenced by many factors. The location and layout of the project are shown in Figure 1.

Related control parameters

The operating water level for two operating units is the same as that for three operating units for the first six pump stations. The relevant design information for the first six pumping stations is shown in Table 1. Additionally, Table 2 shows the actual operating water level control parameters before and after the pumping stations at all levels.

MODEL DEVELOPMENT

Setup of the open-channel transient flow algorithm based on the one-dimensional Saint-Venant equations

The basic problem associated with non-constant gradient flow is determining the variations in hydraulic elements (such as the discharge Q, flow velocity v, water level z or water depth h) along the flow track s over time t. The most commonly used to describe unsteady gradient flows are the partial differential equations of unsteady flow,

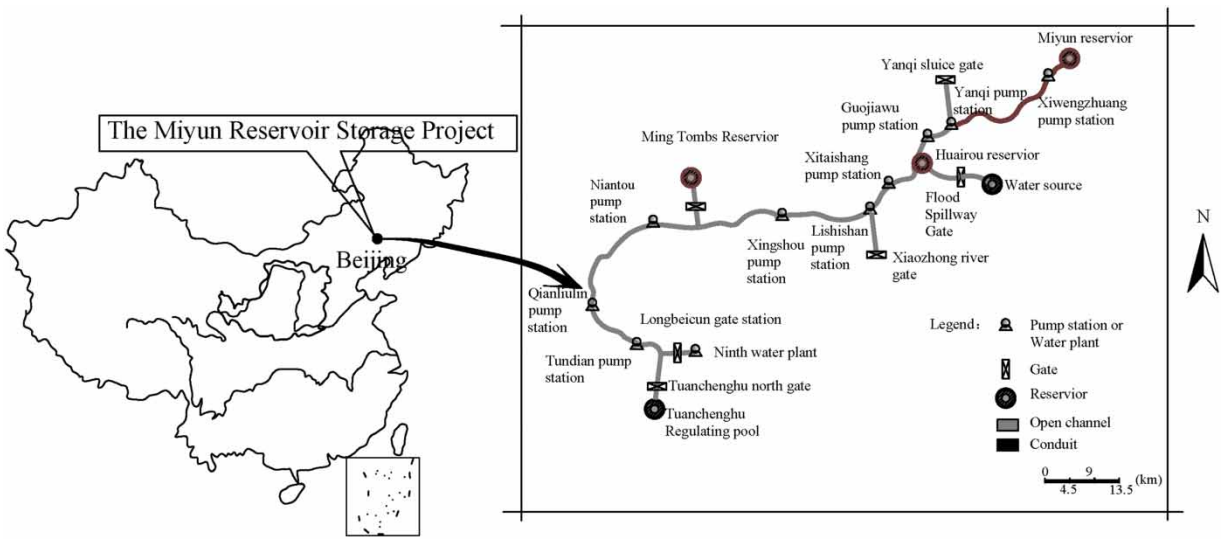

Figure 1 | Location of the study area and layout of the Miyun Reservoir Storage Project.

Table 1 | Pump station design information

Parameter name		Tundian (4 with 1 standby)	Qianliulin (4 with 1 standby)	Niantou (4 with 1 standby)	Xingshou (4 with 1 standby)	Lishishan (4 with 1 standby)	Xitaishang (4 with 1 standby)
Net lift	H_{max} (m)	1.50	2.20	2.45	2.21	2.04	8.18
	H_d (m)	1.08	1.60	2.21	1.97	1.59	6.18
	H_{min} (m)	0.11	1.27	2.06	1.82	1.29	4.31
Pump	Impeller diameter (mm)	1,460	1,460	1,460	1,460	1,460	1,460
	Adjustment method	Blade adjusting	Blade adjusting	Blade adjusting	Blade adjusting	Blade adjusting	Blade adjusting
	Designed net lift (m)	1.08	1.60	2.21	1.97	1.59	6.18
	Unit discharge (m^3/s)	6.67	6.67	6.67	6.67	6.67	6.67
	Pump style	Vertical axial flow	Vertical axial flow	Vertical axial flow	Vertical axial flow	Vertical axial flow	Vertical mixed flow
Motor	Match power (kW)	315	355	400	355	355	1,000
	Rev (r/min)	245	245	245	245	245	290
	Working voltage (kV)	10	10	10	10	10	10

which is referred to as the Saint-Venant equations (Kilic & Anac 2010; Kannan *et al.* 2011).

Continuous equation

$$\frac{\partial A}{\partial t}+\frac{\partial Q}{\partial x}=q \tag{1}$$

Momentum equation

$$\frac{\partial}{\partial t}\left(\frac{Q}{A}\right)+\frac{\partial}{\partial x}\left(\alpha\frac{Q^2}{2A^2}\right)+g\frac{\partial Z}{\partial x}+g(S_f-S_0)=0 \tag{2}$$

where Z is the water level (m), Q is the flow capacity ($m^3\ s^{-1}$), A is the cross-sectional area (m^2), g is the acceleration of gravity ($m\ s^{-2}$), x is the length in the flow direction (m), t is the calculation time (s), q is the lateral inflow or outflow capacity of a unit length of channel ($m^2\ s^{-1}$), α is the correction coefficient of momentum, S_f is the friction gradient, and S_0 is the bottom slope of the canal.

The hydraulic gradient can be calculated according to the flow modulus:

Table 2 | Water level control parameters of the pumping stations based on the actual runtime

Pump station name			Tundian	Qianliulin	Niantou	Xingshou	Lishishan	Xitaishang
One unit operating ($Q = 6.67\ m^3/s$)	Forebay (m)	Min.	48.38	48.60	49.97	51.28	52.23	52.95
		Norm.	48.60	49.16	50.04	51.35	52.28	53.05
		Max.	49.26	49.30	50.12	51.44	52.33	53.10
	Outlet sump (m)	Min.	49.28	50.31	51.48	52.30	53.00	56.23
		Norm.	49.53	50.38	51.55	52.35	53.10	58.71
		Max.	49.69	50.46	51.64	52.40	53.15	60.10
Two units operating ($Q = 13.4\ m^3/s$)	Forebay (m)	Min.	48.38	48.60	49.64	51.02	52.00	52.75
		Norm.	48.60	49.16	49.71	51.09	52.05	52.85
		Max.	49.26	49.30	49.79	51.18	52.10	53.10
	Outlet sump (m)	Min.	49.28	50.31	51.48	52.30	53.00	56.23
		Norm.	49.53	50.38	51.55	52.35	53.10	58.71
		Max.	49.69	50.46	51.64	52.40	53.15	60.10
Three units operating ($Q = 20\ m^3/s$)	Forebay (m)	Min.	48.38	48.60	49.42	50.53	51.30	51.92
		Norm.	48.60	49.16	49.62	50.73	51.50	52.63
		Max.	49.26	49.39	49.72	50.83	51.60	53.91
	Outlet sump (m)	Min.	49.37	50.66	51.78	52.65	52.89	57.23
		Norm.	49.68	50.76	51.83	52.70	53.09	58.81
		Max.	49.88	50.80	51.87	52.74	53.34	60.10

$$S_f = \frac{Q|Q|}{K^2} \tag{3}$$

where K is the modulus of flow ($m^3\ s^{-1}$).

Difference scheme and numerical method

Two commonly used modeling methods are the characteristic line method and the finite difference method, and the validity and accuracy of numerical simulations mainly depends on the meshing approach, the interpolation function of the discrete equation, the initial and boundary conditions and so on. The characteristic line method has a simple and intuitive solution that is physically representative. However, the method has various limitations, such as requiring an irregular grid, producing a low computing efficiency, and requiring interpolation because the calculation position deviates from the calculation grid (Clemmens *et al.* 2005; Devi 2014). Therefore, the Preissmann four-point eccentric lattice difference method, which is a stable, precise and simple method widely used in finite difference schemes, is adopted in this study.

As shown in Figure 2, the value of the differential sum function of mesh eccentricity M at point M is as follows:

$$\begin{aligned} f &= \theta f_U + (1-\theta) f_D \\ &= \theta\left[\psi f_{j+1}^{n+1} + (1-\psi) f_j^{n+1}\right] + (1-\theta)\left[\psi f_{j+1}^{n} + (1-\psi) f_j^{n}\right] \end{aligned} \tag{4}$$

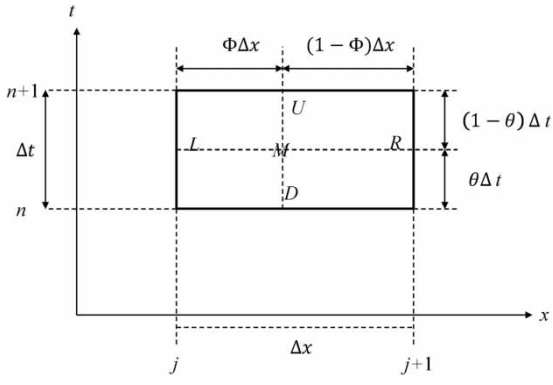

Figure 2 | Schematic diagram of the four-point, time-based eccentric format.

The discretization scheme of the equations over time is given by formula (5).

$$\frac{\partial f}{\partial t} = \frac{f_U - f_D}{\Delta t} = \psi \frac{f_{j+1}^{n+1} - f_{j+1}^{n}}{\Delta t} + (1-\psi)\frac{f_j^{n+1} - f_j^{n}}{\Delta t} \tag{5}$$

The discretization scheme of the continuum equation in space is given by formula (6).

$$\frac{\partial f}{\partial x} = \frac{f_R - f_L}{\Delta x} = \theta \frac{f_{j+1}^{n+1} - f_j^{n+1}}{\Delta x} + (1-\theta)\frac{f_{j+1}^{n} - f_j^{n}}{\Delta x} \tag{6}$$

Additionally, the discretization scheme of the momentum equation in space is as follows:

$$\frac{\partial f}{\partial x} = \phi \frac{f_{j+1}^{n+1} - f_j^{n+1}}{\Delta x} + (1-\phi)\frac{f_{j+1}^{n} - f_j^{n}}{\Delta x} \tag{7}$$

$$S_f = \phi\left[\varphi S_{f,j+1}^{n+1} + (1-\varphi) S_{f,j}^{n+1}\right] + (1-\phi)\left[\varphi S_{f,j+1}^{n} + (1-\varphi) S_{f,j}^{n}\right] \tag{8}$$

where Δx is the spatial step, Δt is the time step, f is the value at eccentric point M, j is the node number of the canal (from 1 to j for $j-1$ canals), n is the number of time steps, θ is the weighted coefficient of time ($0 \le \theta \le 1.0$), ψ is the weighted coefficient of space ($0 \le \psi \le 1.0$), ϕ is the weighted coefficient of time discretization in the continuum equation and φ is the weighted coefficient of the hydraulic gradient in space.

Considering the stability conditions of the Preissmann four-point space-time eccentric scheme, formula (5) is used to discretize time in the continuum and momentum equations, formula (6) is used to discretize space in the continuum equation and formulas (7) and (8) are used to discretize space in the momentum equation.

The updated continuum equation is given in formula (9).

$$\begin{aligned} &\frac{\psi}{\Delta t}\left(A_{j+1}^{n+1} - A_{j+1}^{n}\right) + \frac{1-\psi}{\Delta t}\left(A_j^{n+1} - A_j^{n}\right) + \frac{\theta}{\Delta x}\left(Q_{j+1}^{n+1} - Q_j^{n+1}\right) \\ &+ \frac{1-\theta}{\Delta x}\left(Q_{j+1}^{n} - Q_j^{n}\right) - \theta\left[\psi q_{j+1}^{n+1} + (1-\psi) q_j^{n+1}\right] \\ &- (1-\theta)\left[\psi q_{j+1}^{n} + (1-\psi) q_j^{n}\right] = 0 \end{aligned} \tag{9}$$

Additionally, the momentum equation is shown in formula (10).

$$\begin{aligned}&\frac{\psi}{\Delta t}\left(\frac{Q_{j+1}^{n+1}}{A_{j+1}^{n+1}}-\frac{Q_{j+1}^{n}}{A_{j+1}^{n}}\right)+\frac{1-\psi}{\Delta t}\left(\frac{Q_{j}^{n+1}}{A_{j}^{n+1}}-\frac{Q_{j}^{n}}{A_{j}^{n}}\right)\\&+\frac{\phi}{\Delta x}\left(\frac{1}{2}\left(\frac{\beta_{j+1}^{n+1}Q_{j+1}^{n+1}}{A_{j+1}^{n+1}}\right)^{2}-\frac{1}{2}\left(\frac{\beta_{j}^{n+1}Q_{j}^{n+1}}{A_{j}^{n+1}}\right)^{2}\right)\\&+\frac{1-\phi}{\Delta x}\left(\frac{\beta_{j+1}^{n}}{2}\left(\frac{Q_{j+1}^{n}}{A_{j+1}^{n}}\right)^{2}-\frac{\beta_{j}^{n}}{2}\left(\frac{Q_{j}^{n}}{A_{j}^{n}}\right)^{2}\right)\\&+\frac{\phi g}{\Delta x}\left(y_{j+1}^{n+1}-y_{j}^{n+1}\right)+\frac{(1-\phi)g}{\Delta x}\left(y_{j+1}^{n}-y_{j}^{n}\right)\\&+\phi g\left[S_{f,j+1}^{n+1}+(1-\psi_R)S_{f,j}^{n+1}\right]\\&+(1-\phi)g\left[S_{f,j+1}^{n}+(1-\psi_R)S_{f,j}^{n}\right]=0\end{aligned}\tag{10}$$

It is necessary to apply the loop iteration method to the continuum and momentum equations after discretization because the equations are non-linear. In this paper, the discrete equations are linearized by solving for ΔQ and Δh. In the cyclic solution process, the current value is calculated using the following equations: $h = h^* + \Delta h$ and $Q = Q^* + \Delta Q$, where $h^*$and Q^* are the values of Q and h, respectively, in the previous loop.

By simplifying the linearized continuum equation, the following formula is obtained:

$$a_j\Delta h_j + b_j\Delta Q_j + c_j\Delta h_{j+1} + d_j\Delta Q_{j+1} = p_j \tag{11}$$

where

$$a_{1j}=\frac{(1-\psi)B_j^*}{\Delta t},\ b_{1j}=\frac{-\theta}{\Delta x},\ c_{1j}=\frac{\psi B_{j+1}^*}{\Delta t},\ d_{1j}=\frac{\theta}{\Delta x}$$

and

$$\begin{aligned}e_{1j}=&-\frac{\psi}{\Delta t}(A_{j+1}^*-A_{j+1}^n)-\frac{1-\psi}{\Delta t}(A_j^*-A_j^n)\\&-\frac{\theta}{\Delta x}(Q_{j+1}^*-Q_j^*)-\frac{1-\theta}{\Delta x}(Q_{j+1}^n-Q_j^n)\\&+\theta\left[\psi q_{j+1}^{n+1}+(1-\psi)q_j^{n+1}\right]+(1-\theta)\left[\psi q_{j+1}^{n}+(1-\psi)q_j^{n}\right].\end{aligned}$$

By simplifying the linearized momentum equation, the following formula is obtained:

$$e_{j+1}\Delta h_j + a_{j+1}\Delta Q_j + b_{j+1}\Delta h_{j+1} + c_{j+1}\Delta Q_{j+1} = p_{j+1} \tag{12}$$

where

$$a_{2j}=\frac{(1-\psi)Q_j^*B_j^*}{\Delta t(A_j^*)^2}+\frac{\phi(Q_j^*)^2B_j^*}{\Delta x(A_j^*)^3}-\frac{g\phi}{\Delta x}-2\phi g(1-\varphi)\frac{S_{f,j}^*}{K_j^*}\left(\frac{\partial K}{\partial h}\right)_j^*,$$

$$b_{2j}=\frac{1-\psi}{\Delta tA_j^*}-\frac{\phi Q_j^*}{\Delta x(A_j^*)^2}+2g\phi(1-\varphi)\frac{|Q_j^*|}{(K_j^*)^2},$$

$$c_{2j}=-\frac{\psi Q_{j+1}^*B_{j+1}^*}{\Delta t(A_{j+1}^*)^2}-\frac{\phi(Q_{j+1}^*)^2B_{j+1}^*}{\Delta x(A_{j+1}^*)^3}+\frac{\phi g}{\Delta x}-2g\phi\varphi\frac{S_{f,j+1}^*}{K_{j+1}^*}\left(\frac{\partial K}{\partial h}\right)_{j+1}^*,$$

$$d_{2j}=\frac{\psi}{\Delta tA_{j+1}^*}+\frac{\phi Q_{j+1}^*}{\Delta x(A_{j+1}^*)^2}+2g\phi(1-\varphi)\frac{|Q_j^*|}{(K_{j+1}^*)^2}$$

and

$$\begin{aligned}e_{2j}=&-\frac{\psi}{\Delta t}\left(\frac{Q_{j+1}^*}{A_{j+1}^*}-\frac{Q_{j+1}^n}{A_{j+1}^n}\right)-\frac{1-\psi}{\Delta t}\left(\frac{Q_j^*}{A_j^*}-\frac{Q_j^n}{A_j^n}\right)\\&-\frac{\alpha\phi}{2\Delta x}\left[\left(\frac{Q_{j+1}^*}{A_{j+1}^*}\right)^2-\left(\frac{Q_j^*}{A_j^*}\right)^2\right]=-\frac{\alpha(1-\phi)}{2\Delta x}\\&\left[\left(\frac{Q_{j+1}^n}{A_{j+1}^n}\right)^2-\left(\frac{Q_j^n}{A_j^n}\right)^2\right]-\frac{g\phi}{\Delta x}(h_{j+1}^*-h_j^*)\\&-\frac{g(1-\phi)}{\Delta x}(h_{j+1}^n-h_j^n)-g\phi\left[\varphi S_{f,j+1}^*+(1-\varphi)S_{f,j}^*\right]\\&-g(1-\phi)\left[\varphi S_{f,j+1}^n+(1-\varphi)S_{f,j}^n\right]+gS_0.\end{aligned}$$

By performing differencing techniques and linearizing the Saint-Venant equations using the above difference scheme, two linear forms of formulas (11) and (12) are obtained. The canal is divided into (m-1) small canal units in m sections and 2(m-1) equations with 2m variants. Additionally, 2m equations are coupled with upstream and downstream boundary conditions. Thus, closed algebraic equations are formed, and they can be solved using an

efficient double sweep algorithm. The matrix form of the closed algebraic equations is as follows:

$$AX = D \tag{13}$$

where matrices A, X and D are

$$A = \begin{Bmatrix} a_1 & b_1 & & & & & & \\ a_2 & b_2 & c_2 & d_2 & & & & \\ a_3 & b_3 & c_3 & d_3 & & & & \\ & & a_4 & b_4 & c_4 & d_4 & & \\ & & a_5 & b_5 & c_5 & d_5 & & \\ & & \vdots & \vdots & \vdots & \vdots & & \\ & & & & a_{2m-2} & b_{2m-2} & c_{2m-2} & d_{2m-2} \\ & & & & a_{2m-1} & b_{2m-1} & c_{2m-1} & d_{2m-1} \\ & & & & & & a_{2m} & b_{2m} \end{Bmatrix},$$

$$X = \begin{pmatrix} \Delta h_1 \\ \Delta Q_1 \\ \Delta h_2 \\ \Delta Q_2 \\ \Delta h_3 \\ \vdots \\ \Delta Q_{m-1} \\ \Delta h_m \\ \Delta Q_m \end{pmatrix} \text{ and } D = \begin{pmatrix} e_1 \\ e_2 \\ e_3 \\ e_4 \\ e_5 \\ \vdots \\ e_{2m-2} \\ e_{2m-1} \\ e_{2m} \end{pmatrix}, \text{ respectively.}$$

Boundary condition generalization

Generally, a water delivery system based on cascade pumping stations can be considered a series of hydraulic structures with the system-based boundary conditions at the outer and inner boundaries. The outer boundary condition includes the water level ($Z = f(t)$), flow capacity ($Q = f(t)$), relationship between the water level and discharge ($Q = f(Z)$) and so on. The inner boundaries are based on discontinuous geometric points and the hydraulic characteristics of the channel (or canal). In this study, the discontinuous points include the transition section, areas of inverted siphon flow, pumping stations and other co-dependent structures for which the Saint-Venant equations are not suitable. Combined with the characteristics of open-channel transient flow, the channel module, transition section module, inverted siphon module, pump station module and other modules are developed. The topological relationships between modules are established to facilitate coupling with the control equations and to provide a continuous calculation in space. The generalized relationships between each module are shown in Figure 3.

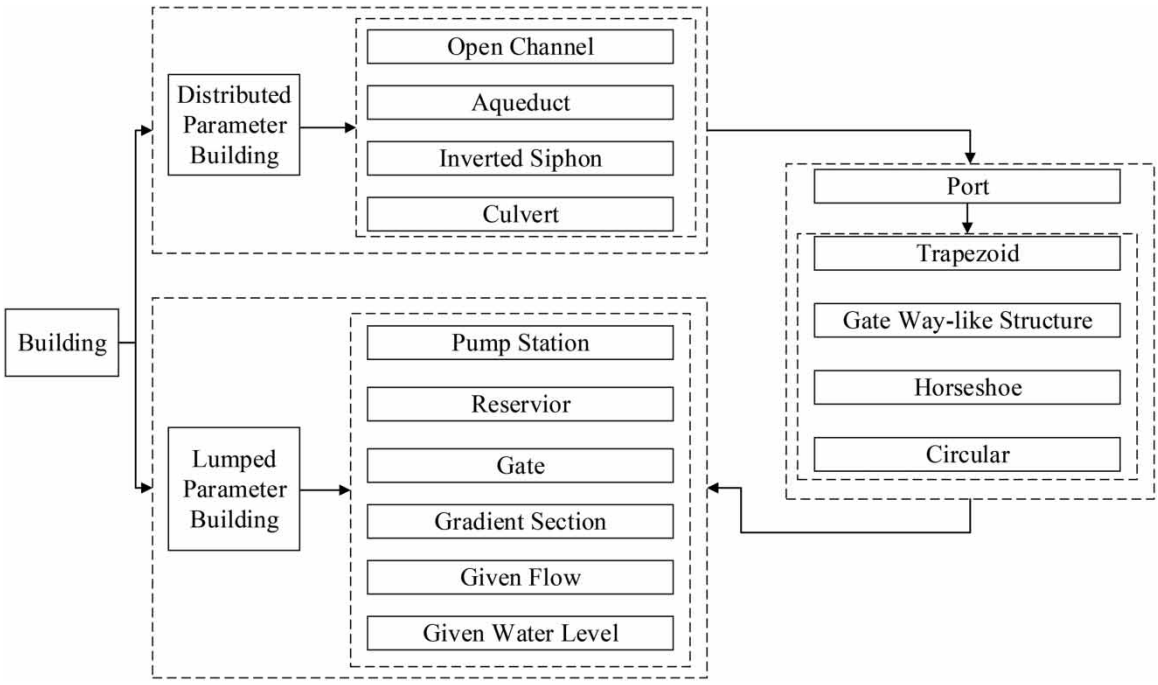

Figure 3 | Schematic diagram of the generalized relationship between each module.

Numerical simulation and model validation

The hydraulic parameters, such as the channel roughness and local head loss coefficient along the structure, used in the design of large-scale water diversion projects, directly affect the hydraulic response characteristics of the water delivery system. The Miyun-Beijing diversion canal has been operated for many years, and seepage prevention and reinforcement measures have only been applied to some parts of the channels. Additionally, the growth of lush plants in the channel is important. The numerical calculation model in this paper is established based on the roughness and local head loss values determined by Wang (2007). The channel roughness value ranged from 0.015–0.04, and the corresponding channel parameters used in the numerical simulations are shown in Table 3.

Through the numerical simulation of the hydraulic transition process of the cascade pumping stations used in the Miyun Reservoir Regulation Project, the accuracy and practicability of the model were validated via a comparison between the actual cross-sectional data from the Miyun-Beijing diversion canal, engineered operating levels and the simulation results. The numerical simulation results are shown in Table 4. The numerical results exhibit satisfactory agreement with the operating levels but are slightly larger than the measured values. With one unit operating, the maximum difference between the calculated water level and observed water level was observed at the outlet of Qianliulin pump station, and the error was 2 cm. With two units operating, the maximum difference between the calculation water level and observed water level was observed at the outlets of Qianliulin and Xingshou pump stations, and the error was 1 cm. Overall, the composite effects of the water surface profile were effectively represented. The numerical model of transient flow developed by combining computer simulation techniques and the one-dimensional Saint-Venant equations meets the research and application needs of this study. It is suitable for research regarding hydraulic transient processes, operation scheduling, and security and stability in the water delivery system of the cascade pumping stations of the South-to-North Water Transfer Project and the Miyun Reservoir Regulation and Storage Project.

RESULTS AND DISCUSSION

Analysis of the response characteristics of the hydraulic transient process under pump switching conditions

The developed hydraulic numerical model was used to evaluate the hydraulic transient process under single and double pump switching conditions (from 11:30 am to 17:30 pm on 28 September, 2015). The water level hydrographs are shown in Figure 4(a)–4(d).

By comparing the simulation results to the observed results, we can see that the overall trends are consistent.

Table 3 | Parameters of the canals

Channel section		Length (km)	Side slope	Bottom width (m)	Coefficient of roughness ($s\ m^{-1/3}$)	Longitudinal slope
North gate of Lake City Mission	Tundian pump station	8.22	1:2–1:2.5	12–20	0.02	0.000058
Tundian pump station	Qianliulin pump station	9.43	1:2.5–1:2.5	20	0.029	0.000058
Qianliulin pump station	Niantou pump station	15.77	1:2.5–1:2.5	20	0.04	0.000062
Niantou pump station	Xingshou pump station	19.29	1:2.5–1:2.5	20	0.026	0.000058
Xingshou pump station	Lishishan pump station	14.4	1:2.5–1:2.5	20	0.016	0.000056
Lishishan pump station	Xitaishang pump station	5.06	1:2.5–1:2.5	20	0.021	0.000056

Table 4 | Simulation results and comparison to the measured results

	One unit operating			Two units operating		
Node name	**Calculated level (m)**	**Observed level (m)**	**Error value (cm)**	**Calculated level (m)**	**Observed level (m)**	**Error value (cm)**
Forebay of Tundian	49.22	49.22	0.00	48.96	48.96	0.00
Outlet sump of Tundian	49.61	49.60	1.00	49.60	49.60	0.00
Forebay of Qianliulin	49.54	49.54	0.00	49.40	49.40	0.00
Outlet sump of Qianliulin	50.35	50.37	2.00	50.55	50.54	1.00
Forebay of Niantou	50.02	50.02	0.00	49.82	49.82	0.00
Outlet sump of Niantou	51.49	51.50	1.00	51.79	51.79	0.00
Forebay of Xingshou	51.35	51.35	0.00	51.40	51.40	0.00
Outlet sump of Xingshou	52.34	52.35	1.00	52.41	52.40	1.00
Forebay of Lishishan	52.27	52.27	0.00	52.20	52.20	0.00
Outlet sump of Lishishan	52.82	52.82	0.00	52.94	52.95	0.00
Forebay of Xitaishang	52.76	52.76	0.00	52.78	52.78	0.00
Outlet sump of Xitaishang	57.96	57.96	0.00	58.74	58.74	0.00

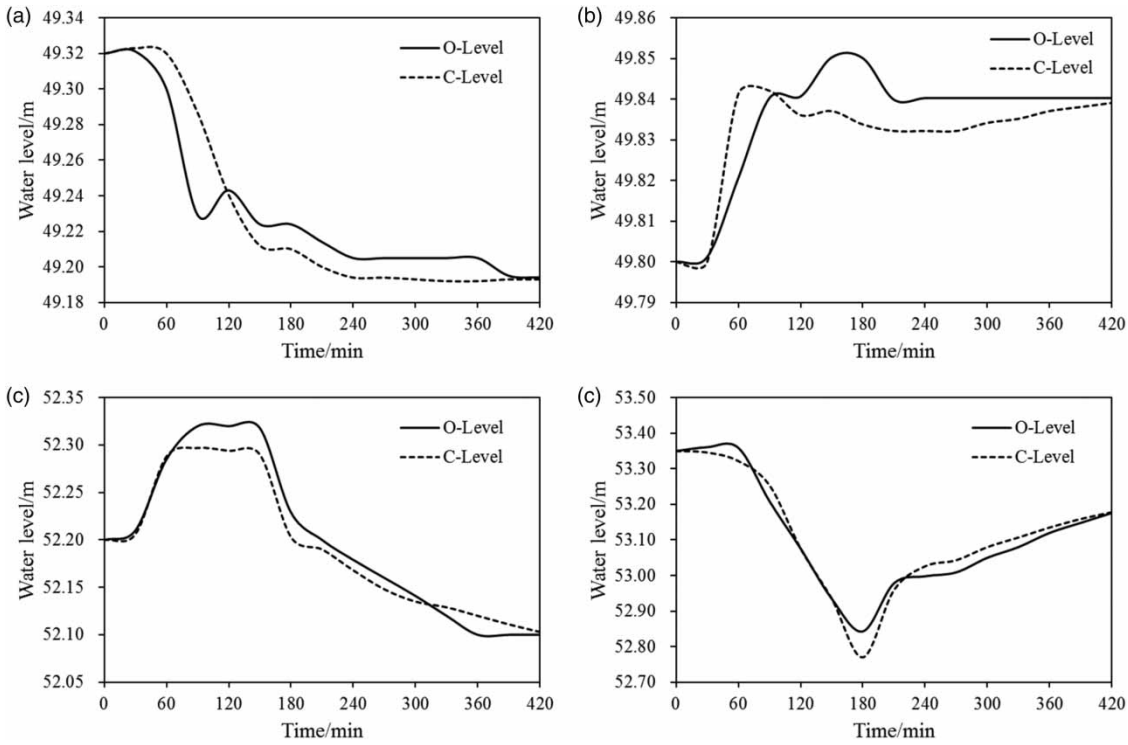

Figure 4 | Simulated result of single and double sets switching events (where O-Level refers to observation values, C- Level refers to calculation values). (a) Water level hydrograph at the inlet pool of Qianliulin pump station. (b) Water level hydrograph at the inlet pool of Niantou pump station. (c) Water level hydrograph at the inlet pool of Lishishan pump station. (d) Water level hydrograph at the inlet pool of Xitaishang pump station.

The maximum decrease in the water level at the inlet pool of Qianliulin pump station was 13.1 cm, and the minimum operating water level was 49.19 m, which did not surpass the minimum limit of the water level (48.60 m). Additionally, the maximum water level error was 5.7 cm.

The maximum increase in the water level at the inlet pool of Niantou pump station was 4.2 cm, and the maximum operating water level was 49.84 m, which did not surpass the maximum limit of the water level (50.12 m). Additionally, the maximum water level error was 2.1 cm.

The maximum increase in the water level at the inlet pool of Lishishan pump station was 9.7 cm, the maximum operating water level was 52.3 m and the maximum decrease in the water level was 19.4 cm. Additionally, the minimum operating water level was 52.10 m, which did not surpass the minimum limit of the water level (52.00 m), and the maximum water level error was 2.8 cm.

The maximum decrease in the water level at the inlet pool of Xitaishang pump station was 58 cm, and the minimum operating water level was 52.77 m, which did not surpass the minimum limit water level (52.75 m). Additionally, the maximum increase in the water level was 40.8 cm, and the maximum operating water level was 53.18 m, which surpassed the maximum limit water level (53.10 m) after 347 min. The maximum water level error was 7.3 cm.

In summary, considering the influence of the large fluctuations in water level under single and double pump unit switching conditions and the water level error, the simulation results are reasonable. By comparing the simulation results to observations, we found that the overall trends in the data were consistent. The water levels exhibited relatively large fluctuations under switching conditions, but the fluctuations were within the designed water level range. To ensure the safety of the channel lining and avoid large fluctuations in the water level, pumping stations should try to establish balanced flow operation throughout the entire system.

Analysis of the response characteristics of the hydraulic transient process during pump shutdown

All operating units shut down at a single-stage pump station in a water delivery system of cascade pump stations

The delivery system from Tundian pump station to Xitaishang pump station is selected as the research extent. At each pump station, three units are in use and one is in reserve. The designed flow capacity is 20 m^3/s, and the initial water level is set as a constant. The developed hydraulic numerical model was used to analyze the hydraulic transient process when all operating units are shut down at a single-stage pump station in a water delivery system of cascade pump stations. The following scenarios were assumed:

Scenario 1: Assuming that the water delivery system undergoes normal operation for 1,400 seconds, all operating units shut down at Qianliulin pump station, and the flow capacity changes from 20 m^3/s to 0.

Scenario 2: Assuming that the water delivery system undergoes normal operation for 1,400 seconds, all operating units shut down at Niantou pump station, and the flow capacity changes from 20 m^3/s to 0.

Scenario 3: Assuming that the water delivery system undergoes normal operation for 1,400 seconds, all operating units shut down at Xingshou pump station, and the flow capacity changes from 20 m^3/s to 0.

Characteristic sections were selected upstream and downstream of the pump station with units shut down. Water level variations upstream and downstream were analyzed under the condition of single-stage pump station shutdown. The water level hydrographs in the characteristic sections upstream and downstream of the selected pump stations are shown in Figures 5–7 for various scenarios.

In scenario 1, if no measures are taken at the upstream or downstream pump stations, the water level upstream will continually increase and the water level downstream will continually decrease after Qianliulin pump station suddenly shuts down. Additionally, the water level of the inlet pool at Qianliulin station will exceed the maximum limit (49.39 m) after shutdown. Moreover, approximately 104 minutes after shutdown, the water level of the outlet pool upstream of the pump station will exceed the maximum limit (49.88 m), but no overtopping phenomenon will occur in the stepped channels. Approximately 220 minutes after shutdown, the water level of the inlet pool downstream of the pump station will surpass the minimum limit (49.42 m), which may cause pump cavitation and vibration phenomena.

In scenario 2, if no measures are taken at the upstream or downstream pump stations, the water level upstream will continually increase and the water level downstream will continually decrease after Niantou pump station suddenly shuts down. The water level of the inlet pool of Niantou

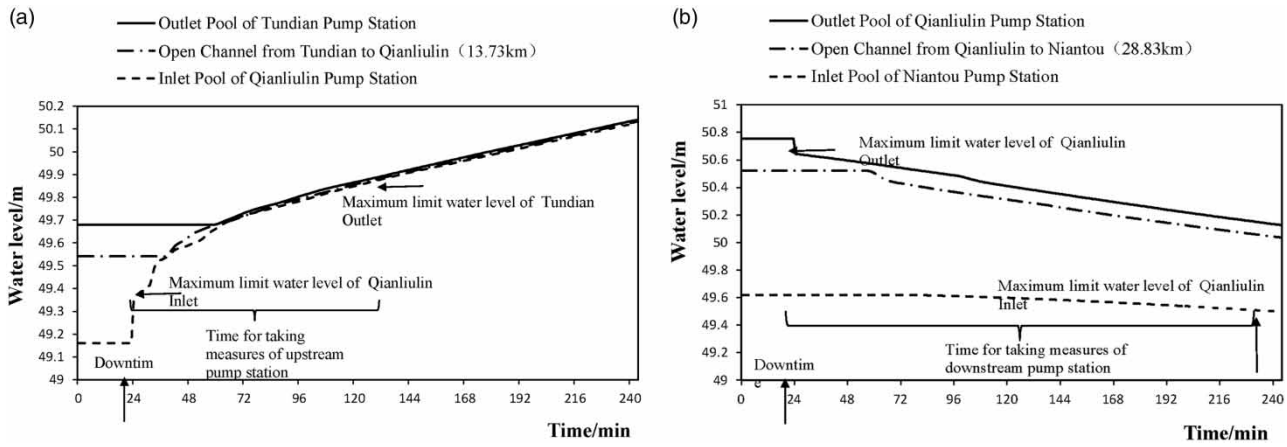

Figure 5 | Scenario 1: stage hydrographs in typical sections upstream and downstream of a pump station that is shut down.

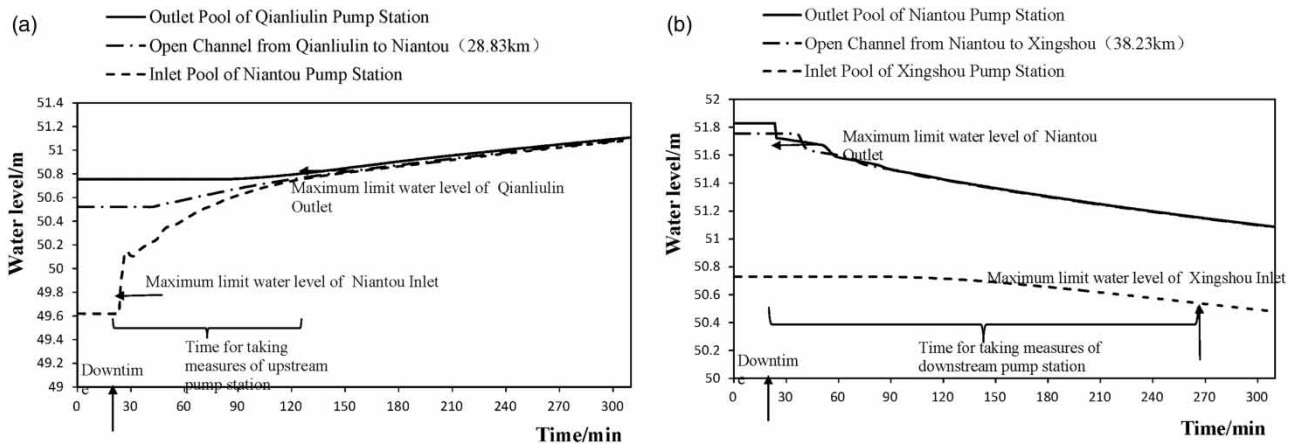

Figure 6 | Scenario 2: stage hydrographs in typical sections upstream and downstream of a pump station that is shut down.

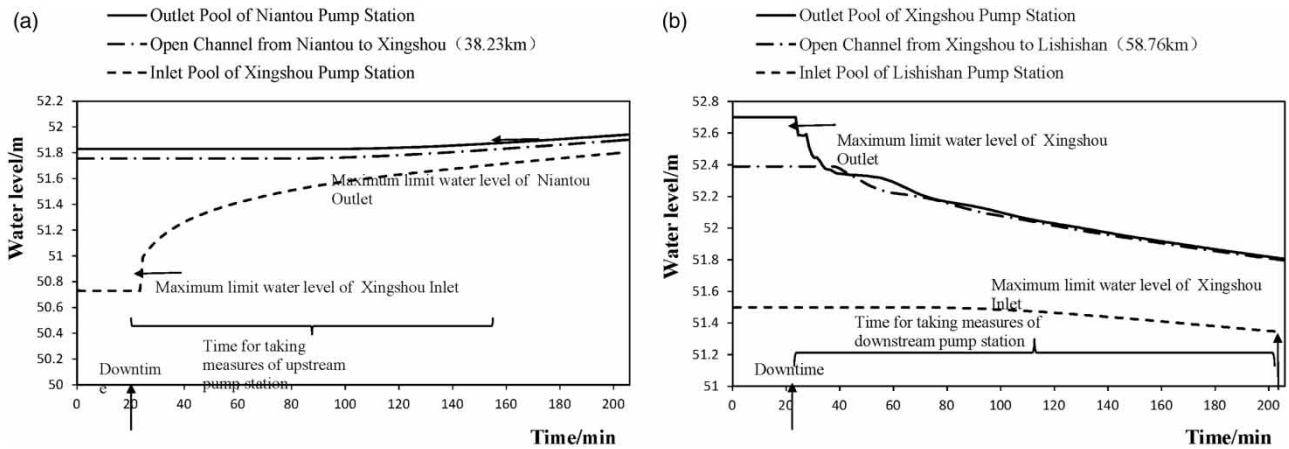

Figure 7 | Scenario 3: stage hydrographs in typical sections upstream and downstream of a pump station that is shut down.

station will exceed the maximum limit (49.72 m) after shutdown. Moreover, approximately 101 minutes after shutdown, the water level of the outlet pool upstream of the pump station will exceed the maximum limit (50.8 m), but no overtopping phenomenon will occur in the stepped channels. Approximately 249 minutes after shutdown, the water level of the inlet pool downstream of the pump station will surpass the minimum limit (50.53 m), which may cause pump cavitation and vibration phenomena.

In scenario 3, if no measures are taken at the upstream or downstream pump stations, the water level upstream will continually increase, and the water level downstream will continually drop after Xingshou pump station suddenly shuts down. The water level of the inlet pool of Xingshou station will exceed the maximum limit (50.83 m) after shutdown. Moreover, approximately 106 minutes after shutdown, the water level of the outlet pool upstream of the pump station will exceed the maximum limit (51.87 m), but no overtopping phenomenon will occur in the stepped channels. Approximately 158 minutes after shutdown, the water level of the inlet pool downstream of the pump station will exceed the minimum limit (51.3 m), which may cause pump cavitation and vibration phenomena.

In conclusion, when a single-stage pump station is operating based on a full load (three pump units), if shutdown occurs, the water levels of the inlet and outlet pools of the pump station will exceed their limits. The cascading pump stations cannot maintain a flow balance under these conditions if no measures are taken at the upstream or downstream pump stations. However, due to the existing storage capacity of the channels, the water levels in the channel sections rise or fall relatively slowly. This creates a certain reaction time for controlling the water delivery system, but there are also differences in reaction times due to the different lengths of channels.

All operating units in a water delivery system of cascade pump stations shut down

The delivery system from Tundian pump station to Xitaishang pump station is selected as the research extent. At each pump station, three units are in use and one is in reserve. We assume that all pump stations in the system use three pump units, and the flow capacity is 20 m^3/s. The initial water level is assigned a constant value. Assuming that the water delivery system undergoes normal operation for 1,400 seconds, all operating units in the water delivery system of cascade pump stations shut down, and the flow capacity changes from 20 m^3/s to 0. The characteristic section includes the outlet pools, the inlet pools of the pump stations of the water delivery system and the open channels between the two pump stations. The water level hydrographs of the characteristic sections after all pump stations are shut down are shown in Figure 8(a)–8(e).

To summarize, when all operating units in the water delivery system of the cascade pump stations are shut down, the hydraulic transition process has the following characteristics:

(1) When the pump stations in an entire system are at full operational capacity (three pump units), after shutdown occurs, the water levels of the inlet and outlet pools of each pump station will undergo relatively severe fluctuations compared to those in open channels. The maximum fluctuation in the water level of the outlet pool of each pump station is 0.22–0.56 m, and the maximum fluctuation in the water level of the inlet pool of each pump station is 0.46–0.97 m. These levels are within the designed water level range.
(2) Among the open channels in the system of cascade pump stations, the water levels in the open channels from Tundian to Qianliulin and from Qianliulin to Niantou exhibited relatively small fluctuations of approximately 0.05–0.06 m. However, the water levels in the open channels from Niantou to Xingshou, from Xingshou to Lishishan and from Lishishan to Xitaishang exhibited relatively large fluctuations of approximately 0.23–0.31 m, but no overtopping occurred in the stepped channels.
(3) The water level fluctuations in the water conveyance system attenuated over time, and the water level in the channel remained stable after a certain time.

CONCLUSIONS

In this study, a mathematical model of the corresponding inner boundary was established that considered open channels, co-dependent structures and control structures. The numerical calculation model of transient flow was developed

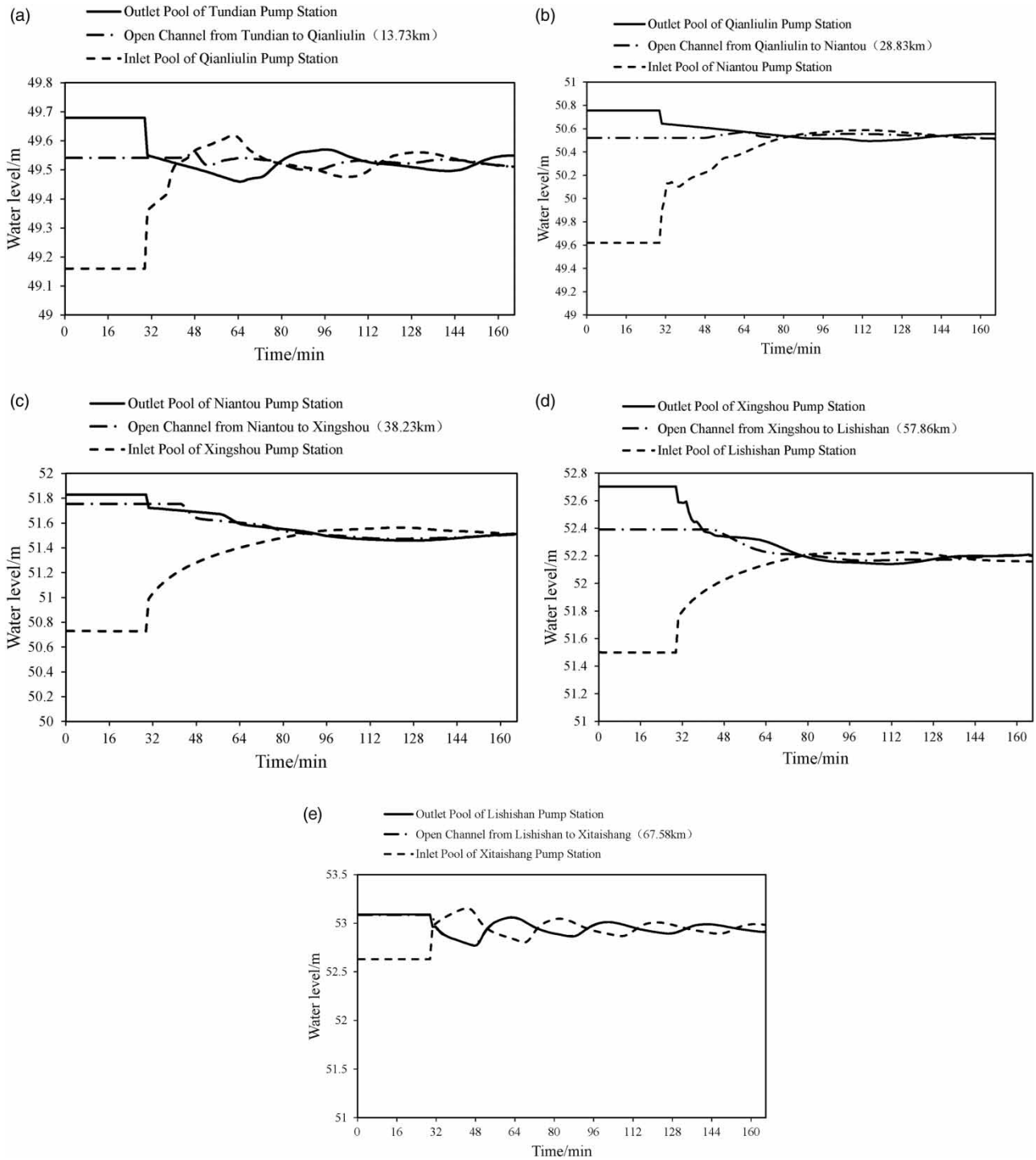

Figure 8 | Stage hydrographs of typical sections upstream and downstream of pump stations after shutdown.

by combining computer simulation techniques and the one-dimensional Saint-Venant equations. This approach is suitable for the water delivery system of cascade pumping stations. The model was used to perform numerical simulations of flow regulation and emergency conditions in the water conveyance system. The numerical model has relatively

high calculation precision, which was suitable for researching the hydraulic transient process of a water delivery system of the cascade pumping stations in the Miyun Reservoir Regulation and Storage Project, and the error in numerical simulations is less than 2 cm. Thus this study provides basic data for the operation and optimization of the water conveyance system and a reference for safe operation of the Miyun Reservoir Storage Project, as well as efficient water delivery.

ACKNOWLEDGEMENTS

The authors gratefully acknowledge the financial assistance from the National Natural Science Foundation of China (NSFC) (No. 51609258). Additionally, we thank the anonymous reviewer whose comments greatly improved the quality of this paper.

REFERENCES

Bolea, Y., Puig, V. & Blesa, J. 2014 Linear parameter varying modeling and identification for real-time control of open-flow irrigation canals. *Environmental Modelling & Software* **53** (C), 87–97.

Burt, C. M. & Gartrell, G. 1993 Irrigation-canal-simulation model usage. *Journal of Irrigation and Drainage Engineering* **119** (4), 631–636.

Chang, J. X., Wang, Y. M. & Huang, Q. 2011 Water dispatch model for middle route of a south-to-north water transfer project in China. *Journal of the American Water Resources Association* **47** (1), 70–80.

Chen, Z. S., Wang, H. M. & Qi, X. T. 2013 Pricing and water resource allocation scheme for the South-to-North water diversion project in China. *Water Resour. Manage.* **27**, 1457–1472.

Clemmens, A. J. 2012 Water-level difference controller for main canals. *Journal of Irrigation and Drainage Engineering* **138** (1), 1–8.

Clemmens, A. J., Bautista, E., Wahlin, B. T. & Strand, R. J. 2005 Simulation of automatic canal control systems. *Journal of Irrigation and Drainage Engineering* **131** (4), 324–335.

Devi, K. 2014 *Numerical Simulation of Free Surface Flow Using lax Diffusive Explicit Scheme*. Department of Civil Engineering National Institute of Technology, Rourkela, pp. 12–43.

Devries, J. J., Tod, I. C. & Hromadka, T. V. 2014 Unsteady canal flow – comparison of simulations with field data. In: *Proceedings, International Symposium, Model-Prototype Correlation of Hydraulic Structures*. American Society of Civil Engineers/International Association for Hydro-Environment Engineering and Research, Colorado Springs, Colorado, pp. 456–465.

Ghumman, A. R., Khan, R. A., Khan, Q. U. Z. & Khan, Z. 2012 Modeling for various design options of a canal system. *Water Resour. Manage.* **26**, 2383–2395.

Gooch, R. S. & Keith, J. 2015 Description and evaluation of program: SNUSM. *Irrigation and Drainage (1991)*, pp. 397–406. ASCE.

Guo, X., Hu, T., Zhang, T. & Lv, Y. 2012 Bilevel model for multi-reservoir operating policy in inter-basin water transfer-supply project. *Journal of Hydrology* **424–425** (4), 252–263.

Han, Y., Hong-Xing, L. V. & Guo-An, Y. U. 2010 Numerical simulation of unsteady flow in irrigation canals with two operating modes. *Journal of Yangtze River Scientific Research Institute* **27** (3), 29–33.

Kannan, N., Jeong, J. & Srinivasan, R. 2011 Hydrologic modeling of a canal-irrigated agricultural watershed with irrigation best management practices: case study. *Journal of Hydrologic Engineering* **16** (9), 746–757.

Kilic, M. & Anac, S. 2010 Multi-objective planning model for large scale irrigation systems: method and application. *Water Resour. Manage.* **24** (12), 3173–3194.

Li, K. B., Shen, B., Li, Z. L. & Sun, N. 2011 Irrigation canal running status analysis and leakage detection method based on unsteady flow simulation. *Transactions of the Chinese Society of Agricultural Engineering* **27** (6), 13–18 (in Chinese).

Li, K. B., Shen, B., Li, Z. L. & Hao, G. R. 2015 Open channel hydraulic response characteristics in irrigation area based on unsteady flow simulation analysis. *Transactions of the Chinese Society of Agricultural Engineering* **31** (10), 107–114 (in Chinese).

Liu, G. Q., Guan, G. H. & Wang, C. D. 2013 Transition mode of long distance water delivery project before freezing in winter. *Journal of Hydroinformatics* **15** (15), 306–320.

Menke, R., Abraham, E., Parpas, P. & Stoianov, I. 2016 Exploring optimal pump scheduling in water distribution networks with branch and bound methods. *Water Resour. Manage.* **30**, 5333–5349.

Pudeh, H. T., Mansouri, M., Haghiabi, A. H. & Yonesi, H. A. 2016 Optimization of hydraulic-Hydrologic complex system of reservoirs and connecting tunnel. *Water Resour. Manage.* **30**, 5177–5191.

Sang, G. Q. 2012 *Research on Operation and Control Optimization of Cascade Pumping Station Water-Delivery System Based on Dynamic Balance*. Shandong University, Jinan, Shandong Province, China, pp. 52–81 (in Chinese).

Serede, I. J., Mutua, B. M. & Raude, J. M. 2014 A review for hydraulic analysis of irrigation canals using HEC-RAS model: a case study of Mwea irrigation scheme, Kenya. *Hydrology* **2** (1), 1–5.

Strelkoff, T. S. & Clemmens, A. J. 1998 Nondimensional expression of unsteady canal flow. *Journal of Irrigation and Drainage Engineering* **124** (1), 59–62.

Wang, K. 2007 *Analysis of Water Delivery Capacity and Hydraulic Response of Middle Route of South to North Water Transfer*

Project. Tsinghua University, Beijing, China, pp. 1–80 (in Chinese).

Wang, G. Q., Ouyang, Q., Zhang, Y. D., Wei, J. H. & Zhang, Z. Y. 2009 *Water Diversion Project in the World.* Science Press, Beijing, pp.100–300 (in Chinese).

Water Conservancy Planning Design and Research Institute of Beijing 2013 *Preliminary Design Report of the Incoming Water From South-to-North Water Transfer Project into the Miyun Reservoir Regulation and Storage Project*. Water Conservancy Planning Design and Research Institute of Beijing, Beijing, China, pp. 1–206 (in Chinese).

Yang, K. L. 2016 Review and frontier scientific issues of hydraulic control for long distance water diversion. *Journal of Hydraulic Engineering* **47**, 424–435 (in Chinese).

Zhang, C. & Zhang, S. D. 2011 Research on the characteristic of hydraulic response of large water diversion system under the control of gates. *Journal of Basic Science and Engineering* **19** (S1), 98–107.

Zhang, C., Fu, X. D. & Wang, G. Q. 2007 One-dimensional numerical model for unsteady flows in long-route open channel with complex inner boundary conditions. *South-to-North Water Transfers and Water Science & Technology* **5** (6), 16–20. doi: 10.13476/j.cnki.nsbdqk.2007.06.006.

Zhang, S. H., Liu, Q. C., Bai, M. J. & Xu, J. D. 2013 Unsteady water flow numerical model for irrigation final canal system based on scalar finite-volume method. *Journal of Irrigation and Drainage* **32** (3), 1–5.

Zhang, C., Zheng, L. S. & Qian, J. 2014 Numerical modeling research and application on the middle route of South-to-North water diversion project in China. In: *Proceedings of the 7th International Symposium on Environmental Hydraulics*, Singapore.

Zhang, C., Zheng, L. S. & Ni, C. F. 2015 Hydraulic response of the water diversion system to the synchronous operation of All gates. *Journal of Basic Science and Engineering* (s1), 102–109.

Zhao, L. H. & Xu, L. Z. 2012 Hydrological information coupling for irrigation district based on numerical simulation of open channel unsteady flows. *Journal of Hydraulic Engineering* **43**, 537–544 (in Chinese).

First received 20 February 2017; accepted in revised form 21 September 2017. Available online 17 November 2017